

## Expression of Low Voltage-Activated $\text{Ca}^{2+}$ Channels in *Xenopus* Oocytes

LEE, JUNG-HA\* AND DONG-PYO HAN

Department of Life Science, Sogang University, Seoul 121-742, Korea

Received: January 26, 2001

Accepted: June 6, 2001

**Abstract** Low-threshold T-type  $\text{Ca}^{2+}$  channels are distinctive voltage-operated gates for external  $\text{Ca}^{2+}$  entry around a resting membrane potential due to their low voltage activation. These phenomena have already been extensively studied due to their relevance in diverse physiological functions. Recently, three T-type  $\text{Ca}^{2+}$  channel  $\alpha_1$  subunits were cloned and their biophysical properties were characterized after expression in mammalian expression systems. In this study,  $\alpha_{1G}$  and  $\alpha_{1H}$  low-threshold  $\text{Ca}^{2+}$  channels were expressed and characterized in *Xenopus* oocytes after adding 5' and 3' untranslated portions of a *Xenopus*  $\beta$  globin to improve their expression levels. The added portions dramatically enhanced the expression levels of the  $\alpha_{1G}$  and  $\alpha_{1H}$  T-type channels. When currents were recorded in 10 mM  $\text{Ba}^{2+}$  as the charge carrier, the activation thresholds were about  $-60$  mV, peak currents appeared at  $-20$  mV, and the reversal potentials were between  $+40$  and  $+45$ . The activation time constants were very similar to each other, while the inactivation time constants of the  $\alpha_{1G}$  currents were smaller than those of  $\alpha_{1H}$ . Taken together, the electrophysiological properties of the  $\alpha_{1G}$  and  $\alpha_{1H}$  channels expressed in *Xenopus* oocytes were similar to the previously reported characteristics of low-threshold  $\text{Ca}^{2+}$  channel currents.

**Key words:** Low-threshold  $\text{Ca}^{2+}$  channel, T-type, *Xenopus laevis*, expression, electrophysiology

The activation of voltage-dependent  $\text{Ca}^{2+}$  channels (VDCCs) by depolarized membrane potentials allows external  $\text{Ca}^{2+}$  influxes into cytoplasm. An increased calcium concentration in cytoplasm plays essential roles in diverse physiological functions, such as muscle contraction, neurotransmitter release from pre-synaptic terminals, hormone secretion from endocrine systems, modulation of enzyme activation, and gene expression [8].

VDCCs can be classified into high voltage-activated (HVA)  $\text{Ca}^{2+}$  channels and low voltage-activated (LVA)  $\text{Ca}^{2+}$  channels based on their thresholds for activation. HVA  $\text{Ca}^{2+}$  channels open in response to potentials higher than  $-30$  mV,

while LVA  $\text{Ca}^{2+}$  channels initiate opening around resting membrane potentials of  $-60$  to  $-70$  mV [8, 9, 18].

Compared to HVA  $\text{Ca}^{2+}$  channels, LVA  $\text{Ca}^{2+}$  channels can be further characterized according to the following electrophysiological properties: (i) inactivation at lower voltages, (ii) transient kinetics due to fast inactivation, (iii) a criss-crossing pattern of traces elicited by a current-voltage protocol, (iv) slower deactivation detected as a slowly decaying tail current, (v) tiny single channel conductance, and (vi) high sensitivity to mibefradil [1, 2, 7, 16, 17, 18, 20]. Related to their specific characteristics, T-type  $\text{Ca}^{2+}$  channels can contribute to diverse physiological functions by triggering a  $\text{Ca}^{2+}$  influx under the following conditions: (i) around resting membrane potentials due to their low threshold for channel activation, (ii) during tail currents of action potentials due to their slow deactivation processes, and (iii) after the recovery of T-type channels by hyperpolarization, such as inhibitory post-synaptic potentials (IPSPs) in thalamus, which is known as post-anodal exaltation [9, 22].

Until now, seven subtypes of HVA  $\text{Ca}^{2+}$  channel  $\alpha_1$  subunits ( $\alpha_{1S}$ ,  $\alpha_{1C}$ ,  $\alpha_{1D}$ ,  $\alpha_{1F}$ ,  $\alpha_{1A}$ ,  $\alpha_{1B}$ , and  $\alpha_{1E}$ ) have been cloned. Recently, Perez-Reyes and his colleagues cloned and expressed three members of low-threshold  $\text{Ca}^{2+}$  channel  $\alpha_1$  subunits ( $\alpha_{1G}$ ,  $\alpha_{1H}$ , and  $\alpha_{1I}$ ). The recorded currents shared similar biophysical and pharmacological properties with native T-type  $\text{Ca}^{2+}$  currents [4, 14, 19]. All three T-type channels were expressed in HEK293 cells and their general biophysical properties compared [11, 14].

In this study, the rat  $\alpha_{1G}$  and the human  $\alpha_{1H}$  were expressed in *Xenopus* oocytes and their currents recorded using the two-electrode voltage clamp method. The expressed currents of the  $\alpha_{1G}$  and the  $\alpha_{1H}$  channels displayed typical electrophysiological properties of T-type calcium channel currents.

## MATERIALS AND METHODS

### Materials

The cloning of rat  $\alpha_{1G}$  and human  $\alpha_{1H}$  cDNA was reported previously [4, 19]. To improve their expression in *Xenopus*

\*Corresponding author  
Phone: 82-2-705-8791; Fax: 82-2-704-3601;  
E-mail: jhleem@ccs.sogang.ac.kr

oocytes, each cDNA was subcloned into pGEM-HEA, which contained 5' and 3' untranslated portions from a *Xenopus*  $\beta$  globin gene [3, 15]. The rat  $\alpha_{1G}$  excised from pSP72 by *EcoRV* was then blunt-end ligated into pGEM-HEA which was opened by *SmaI*. To subclone the human  $\alpha_{1H}$  cDNA into pGEM-HEA, the  $\alpha_{1H}$  cDNA pcDNA3 was digested with *EcoRV* and *BspEI*, then *BspEI* and *XbaI*. Both fragments were ligated into *SmaI*- and *XbaI*-digested pGEM-HEA. The female *Xenopus laevis* was purchased from Xenopus I (Dexter, MI, U.S.A.). Most chemicals used in this study were purchased from Sigma (St Louis, MO, U.S.A.).

### Expression and Electrophysiological Recording of T-Type Channels

The capped cRNAs were synthesized based on linearized plasmids using T7 RNA polymerase according to the manufacturer's protocol (Ambion, Austin, TX, U.S.A.). To synthesize cRNA, the  $\alpha_{1G}$ -pGEM-HEA construct or the  $\alpha_{1H}$ -pGEM-HEA construct was linearized with *AflIII* or *BfiI*. The synthesized cRNAs were then quantified spectrophotometrically.

Several ovary lobes were removed surgically from a female *Xenopus laevis* anesthetized by 0.1% of an ethyl 3-aminobenzoate solution. The ovary lobes were transferred into a  $Ca^{2+}$ -free OR solution (82.5 mM NaCl, 2.5 mM KCl, 1 mM  $MgCl_2$ , 5 mM N-hydroxyethylpiperazine-N'-ethanesulfonic acid (HEPES), pH 7.6-adjusted with 1 M NaOH, autoclaved, then supplemented with gentamicin sulfate). The lobes were then manually torn into small clusters of about 10 oocytes. The oocytes were defolliculated by shaking in a  $Ca^{2+}$ -free solution containing 2 mg/ml collagenase (Type IA, Sigma, U.S.A.). Defolliculated oocytes (stage V-VI) in good condition were manually selected under a microscope and then incubated in an SOS solution (100 mM NaCl, 2 mM KCl, 1.8 mM  $CaCl_2$ , 1 mM  $MgCl_2$ , 5 mM HEPES, pH 7.6-adjusted with 1 M NaOH, 2.5 mM of pyruvate, and 50 mg/ml of gentamicin sulfate) at 18°C for several hours or overnight for recovery. A series of different concentrations of cRNAs were injected into the oocytes using a Drummond Nanoject pipette injector (Parkway, PA) attached to a Narishige micromanipulator (Tokyo, Japan) under a dissecting microscope. The recordings were performed 5 days after the injection.

### Electrophysiology of T-Type Channels Expressed in Oocytes

The two-electrode voltage clamp method was applied to measure the currents from the oocytes injected with the cloned T-type channel cRNA. Glass electrodes were pulled from the capillaries (Cat. # 6010, A-M systems, Everett, WA, U.S.A.) using a Model P-97 pipette puller (Sutter, Instrument Co., Novato, CA, U.S.A.). The tips of the voltage and current electrodes were broken to become

0.3–1.0 M $\Omega$  when filled with 1% agarose melted in a 3 M KCl solution.

The oocytes were impaled in an SOS solution (100 mM NaCl, 2 mM KCl, 1.8 mM  $CaCl_2$ , 1 mM  $MgCl_2$ , 5 mM HEPES, 2.5 mM pyruvic acid, and 50 mg/l gentamicin sulfate). Next, they were voltage-clamped using a two-electrode voltage clamp amplifier (OC-725B, Warner Instrument Corp.). After adjusting the clamping speed, the currents were measured in an SOS medium by a series of depolarization voltage steps from a holding potential of -90 mV. To measure the  $Ca^{2+}$  channel currents, the bathing solution (SOS) was exchanged with a 10 mM  $Ba^{2+}$  solution (10 mM  $Ba(OH)_2$ , 90 mM NaOH, 1 mM KOH, 5 mM HEPES, adjusted to pH 7.4 with methanesulfonic acid).

The data were collected at 5 kHz using a pClamp 6 software (Axon Instrument, Foster City, CA, U.S.A.) via a Digidata 1200 A/D converter (Axon Instrument, Foster City, CA, U.S.A.), then filtered at 1 kHz (#902 Frequency Devices, Haverhill, MA, U.S.A.). The experiments were performed at room temperature (20–22°C).

## RESULTS AND DISCUSSION

The initial expression and electrophysiological characterization of the rat  $\alpha_{1G}$  T-type  $Ca^{2+}$  channels were performed in *Xenopus* oocytes [19]. However, continuous studies of the T-type channel have been hampered by its low expression level in *Xenopus* oocytes. Furthermore, when an attempt was made to express the human  $\alpha_{1H}$  in oocytes, no channel currents were detected (Cribbs and Lee, unpublished data). This was the reason why the  $\alpha_{1H}$  was initially expressed and characterized in HEK 293 cells [4].

Here, the first issue was to examine whether the expression levels of the cloned T-type channels measured by the peak current amplitudes increased proportionally to the injected amounts of the T-type channel cRNA. The mean current amplitude was enhanced proportionally to the amount of injected  $\alpha_{1G}$  cRNA, yet even 100 ng of  $\alpha_{1G}$  cRNA evoked relatively small currents (263±160 nA, mean±SED) (Fig. 1A). However, in the case of human  $\alpha_{1H}$ , no currents were detected in *Xenopus* oocytes, regardless of the injected amount of cRNA (Fig. 1B). For example, an injection of 50 ng cRNA did not produce any detectable currents in oocytes.

To enhance the expression levels of the two T-type calcium channels in *Xenopus* oocytes, each cDNA was subcloned into pGEM-HEA which contained 5' and 3' untranslated portions from a *Xenopus*  $\beta$  globin gene [15]. Surprisingly, 3 ng of the modified  $\alpha_{1G}$  cRNA added to the untranslated portions of a *Xenopus*  $\beta$  globin gene produced robust currents (1305±696 nA, mean±SED, n=5–12), thereby indicating that the 5' and 3' additional sequences increased the expression of  $\alpha_{1G}$  cRNA about 50 fold. Although the

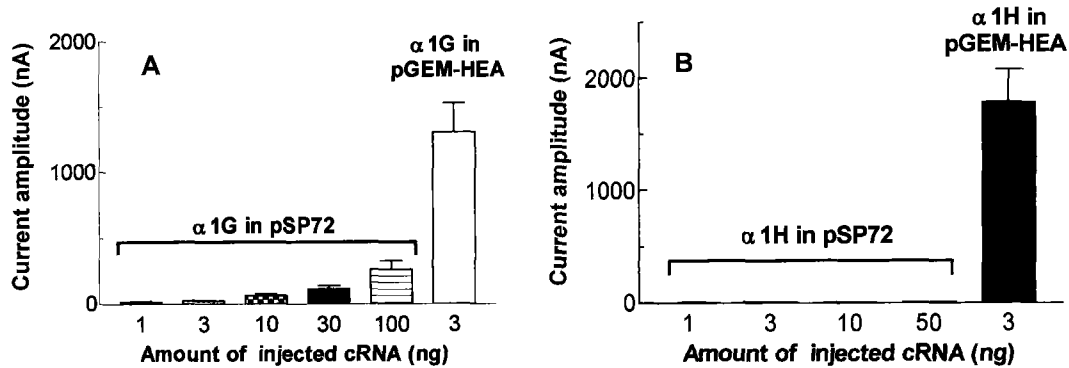


**Fig. 1.** Peak current amplitudes versus injected T-type channel cRNA amounts.

A series of test pulses from a holding potential of  $-90$  mV were applied to measure the current-voltage relationships. The peak current amplitudes measured at  $-20$  mV were averaged and displayed as bar graphs (mean $\pm$ SEM,  $n=5-12$ ). Although the cRNA made from rat  $\alpha_{1G}$  in a pSP72 vector was generally expressed in low levels, these expression levels were increased relative to the injected cRNA amounts. Comparatively, the expression of rat  $\alpha_{1G}$  tagged with the untranslated portions was detected as robust currents (A). No expression of the original human  $\alpha_{1H}$  in pSP72 was detected in *Xenopus* oocytes. The addition of the untranslated portions to the human  $\alpha_{1H}$  rescued the expression of  $\alpha_{1H}$  channels in the oocytes (B).

specific roles of the attached sequences remain to be identified, the enhanced expression by the added sequences suggests that the 5' and 3' sequences may have acted as signal sequences for a better translation in the ribosomes.

The original  $\alpha_{1H}$  was not expressed in the oocytes, but 3 ng of  $\alpha_{1H}$  cRNA containing the  $\beta$  globin portions were

expressed as huge currents in oocytes ( $1,781\pm 710$  nA) (Fig. 1B). This result indicated that the untranslated sequences facilitated the translation processes of the human  $\alpha_{1H}$  cRNA in the oocytes.

Representative  $\alpha_{1G}$  and  $\alpha_{1H}$  currents evoked by a series of tested potentials from a holding potential of  $-90$  mV are

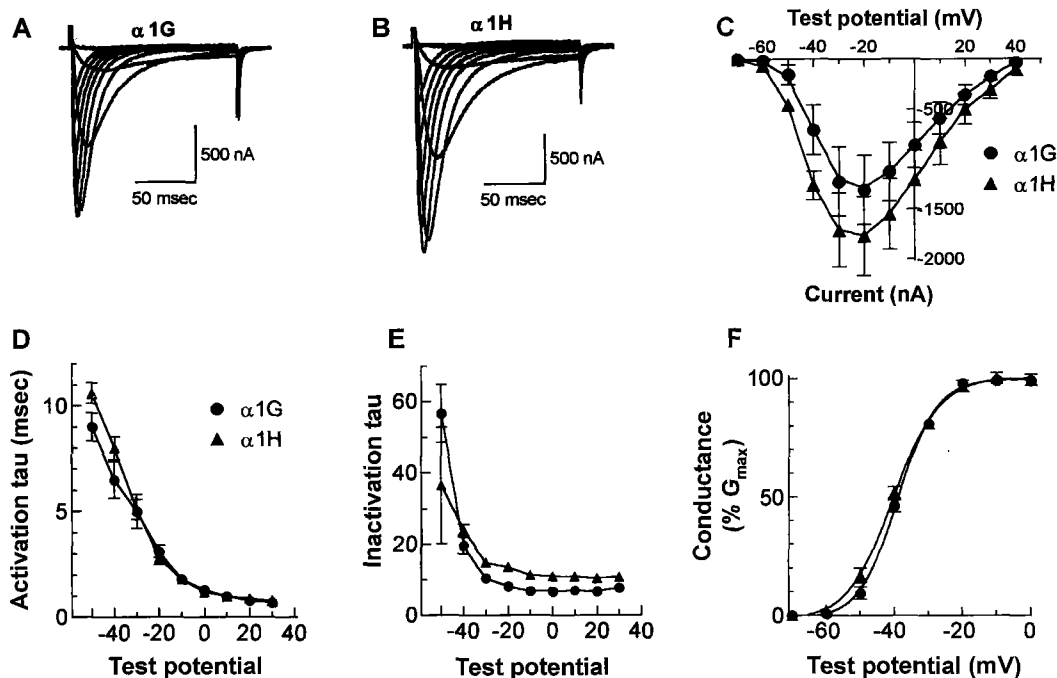


**Fig. 2.** Characteristics of rat  $\alpha_{1G}$  and human  $\alpha_{1H}$  T-type calcium channels expressed in *Xenopus* oocytes.

The current traces were evoked by a series of tests ranging from  $-70$  to  $+40$  mV, from a holding potential of  $-90$  mV. Three ng of cRNA of the  $\alpha_{1G}$  or the  $\alpha_{1H}$  channels was well expressed and their representative traces are shown (A, B). The average current-voltage relationships of the rat  $\alpha_{1G}$  and human  $\alpha_{1H}$  T-type calcium channels were plotted (C). The activation and inactivation time constants of the  $\alpha_{1G}$  and  $\alpha_{1H}$  T-type currents were obtained from fitting each current trace with two exponential curves. The average values of the activation and inactivation time constants of the  $\alpha_{1G}$  and  $\alpha_{1H}$  currents were plotted against test potentials (D, E). The voltage-dependency of the channel activation was compared between the  $\alpha_{1G}$  and  $\alpha_{1H}$  channels using chord conductance. The chord conductance was obtained from dividing the current amplitudes by the driving forces (=apparent reversal potentials-test potentials), normalized to the peak conductance obtained, averaged, and then plotted against the test potentials. The smooth curves were from fitting the plotted data with the Boltzmann equation.

displayed in Fig. 2A. The mean current amplitudes were plotted against the test potentials (Fig. 2B, mean $\pm$ SEM, n=5–12). Both  $\alpha_{1G}$  and  $\alpha_{1H}$  currents began to be detected as inward currents at a test potential of  $-60$  mV, suggesting that their activation threshold was around  $-60$  mV in a  $10$  mM  $Ba^{2+}$  solution. The activation and inactivation kinetics of the currents were accelerated by increased test potentials, displaying a criss-cross pattern between the currents evoked by the voltage protocol. The peak currents were detected at  $-20$  mV. The  $\alpha_{1G}$  and  $\alpha_{1H}$  currents were both reversed between  $+40$  mV and  $+45$  mV, thereby suggesting that the cloned low-threshold  $Ca^{2+}$  channels had less selectivity for  $Ba^{2+}$  than other cloned HVA  $Ca^{2+}$  channels, such as  $\alpha_{1C}$ , where the reversal potential is around  $+65$  mV.

The activation and inactivation time constants of each current were estimated after fitting the recorded trace with two exponential curves. The average values of the activation and inactivation time constants were plotted against test potentials (mean $\pm$ SEM, n=5–12, Figs. 2D, 2E). Both of the parameters were slow in their low voltage range, and became faster as the test potentials were increased. There was no significant difference between the average activation time constants of the rat  $\alpha_{1G}$  and human  $\alpha_{1H}$  currents. Similar to the activation kinetics, the inactivation rate of the rat  $\alpha_{1G}$  and human  $\alpha_{1H}$  currents also displayed a voltage-dependent acceleration. The currents were inactivated slowly within a low voltage range, yet the inactivation kinetics became faster relative to the test potentials. At a potential range higher than  $-30$  mV, the inactivation time constants (7 msec) of the  $\alpha_{1G}$  currents were significantly smaller than those of  $\alpha_{1H}$  (10 msec) (Fig. 2E). The chord conductances of the  $\alpha_{1G}$  and the  $\alpha_{1H}$  channels were plotted to compare their voltage dependency for activation (Fig. 2F). In a  $10$  mM  $Ba^{2+}$  solution, the  $V_{0.5}$  (the midpoint of activation) of the  $\alpha_{1G}$  channels was  $-39.9$  mV and the slope factor was  $5.7$  (n=10), while the  $V_{0.5}$  of the  $\alpha_{1H}$  was  $-40.4$  mV and the slope factor was  $6.6$  (n=6). When compared with the  $\alpha_{1G}$  channels, the  $\alpha_{1H}$  channels tended to exhibit a slightly lower  $V_{0.5}$  and faster slope factor, yet there was no significant difference between the values.

As previously reported [11, 14], the general biophysical properties of rat  $\alpha_{1G}$  and human  $\alpha_{1H}$ , including their thresholds, potentials evoking peak currents, and reversal potentials were similar to each other. However, the inactivation kinetics of rat  $\alpha_{1G}$  were faster than those of human  $\alpha_{1H}$ .

This report compared the expression levels and biophysical properties of rat  $\alpha_{1G}$  and human  $\alpha_{1H}$  and they were compared in oocytes before and after adding 5' and 3' untranslated portions of *Xenopus*  $\beta$  globin cDNA. The results demonstrated that the untranslated portions obviously increased the expression levels of the cloned T-type channels in *Xenopus* oocytes, thereby suggesting that *Xenopus* oocytes can be used as an excellent expression system for their electrophysiological and biochemical characterization

of cloned T-type channels. Accordingly, this method using  $\beta$  globin sequences can also be applied to improve the expression of other foreign proteins in *Xenopus* oocytes. The idea that expression levels of interesting proteins can be improved by addition of untranslated sequences which might be applied to other expression systems such as microorganisms or mammalian cells [10, 21].

## Acknowledgments

The authors would like to thank Drs. Edward Perez-Reyes and Leanne Cribbs for their help. This study was supported by a grant of the Korea Health 21 R&D Project, Ministry of Health & Welfare, Republic of Korea (HMP-00-B-21400-0054).

## REFERENCES

1. Armstrong, C. M. and D. R. Matteson. 1985. Two distinct populations of calcium channels in a clonal line of pituitary cells. *Science* **227**: 65–67.
2. Carbone, E. and H. D. Lux. 1984. A low voltage-activated, fully inactivating Ca channel in vertebrate sensory neurons. *Nature* **310**: 501–502.
3. Chuang, R. S., H. Jaffe, L. Cribbs, E. Perez-Reyes, and K. J. Swartz. 1998. Inhibition of T-type voltage-gated calcium channels by a new scorpion toxin. *Nat. Neurosci.* **1**: 668–674.
4. Cribbs, L. L., J.-H. Lee, J. Yang, J. Satin, Y. Zhang, A. Daud, J. Barclay, M. P. Williamson, M. Fox, M. Rees, and E. Perez-Reyes. 1998. Cloning and characterization of  $\alpha_{1H}$  from human heart, a member of the T-type calcium channel gene family. *Circ. Res.* **83**: 103–109.
5. Freise, D., B. Held, U. Wissenbach, A. Pfeifer, C. Trost, N. Himmerkus, U. Schweig, M. Freichel, M. Biel, F. Hofmann, M. Hoth, and V. Flockerzi. 2000. Absence of the gamma subunit of the skeletal muscle dihydropyridine receptor increases L-type  $Ca^{2+}$  currents and alters channel inactivation properties. *J. Biol. Chem.* **275**: 14476–14481.
6. Gao, B., Y. Sekido, A. Maximov, M. Saad, E. Forgacs, F. Latif, M. H. Wei, M. Lerman, J.-H. Lee, E. Perez-Reyes, I. Bezprozvanny, and J. D. Minna. 2000. Functional properties of a new voltage-dependent calcium channel  $\alpha(2)\delta$  auxiliary subunit gene. *J. Biol. Chem.* **275**: 12237–12242.
7. Gomora, J. C., L. Xu, J. C. Enyeart, and J. Enyeart. 2000. Effect of mibefradil on voltage-dependent gating and kinetics of T-type  $Ca^{2+}$  channels in cortisol-secreting cells. *J. Pharmacol. Exp. Ther.* **292**: 96–103.
8. Hille, B. 1992. *Ion Channels of Excitable Membranes*. 2<sup>nd</sup> ed., Sinauer Associates, Inc., Sunderland, MA, U.S.A.
9. Huguenard, J. R. 1996. Low-threshold calcium channels in central nervous system neurons. *Annu. Rev. Physiol.* **58**: 329–348.

10. Kim, Y. K., D.-Y. Yu, H. A. Kang, S. Yoon, and B. H. Chung. 1999. Secretory expression of human  $\alpha_{s1}$ -casein in *Saccharomyces cerevisiae*. *J. Microbiol. Biotechnol.* **9**: 196–200.
11. Klockner, U., J.-H. Lee, L. L. Cribbs, A. Daud, J. Hescheler, A. Pereverzev, E. Perez-Reyes, and T. Schneider. 1999. Comparison of the  $\text{Ca}^{2+}$  currents induced by expression of three cloned  $\alpha_1$  subunits,  $\alpha_{1G}$ ,  $\alpha_{1H}$  and  $\alpha_{1D}$ , of low-voltage-activated T-type  $\text{Ca}^{2+}$  channels. *Eur. J. Neurosci.* **11**: 4171–4178.
12. Klugbauer, N., L. Lacinova, E. Marais, M. Hobom, and F. Hofmann. 1999. Molecular diversity of the calcium channel  $\alpha_2\delta$  subunit. *J. Neurosci.* **19**: 684–691.
13. Lambert, R. C., F. McKenna, Y. Maulet, E. M. Talley, D. A. Bayliss, L. L. Cribbs, J.-H. Lee, E. Perez-Reyes, and A. Feltz. 1998. Low-voltage-activated  $\text{Ca}^{2+}$  currents are generated by members of the CavT subunit family ( $\alpha_{1G}/H$ ) in rat primary sensory neurons. *J. Neurosci.* **18**: 8605–8613.
14. Lee, J.-H., A. N. Daud, L. L. Cribbs, A. E. Lacerda, A. Pereverzev, U. Klockner, T. Schneider, and E. Perez-Reyes. 1999. Cloning and expression of a novel member of the low voltage-activated T-type calcium channel family. *J. Neurosci.* **19**: 1912–1921.
15. Liman, E. R., J. Tytgat, and P. Hess. 1992. Subunit stoichiometry of a mammalian  $\text{K}^+$  channel determined by construction of multimeric cDNAs. *Neuron* **9**: 861–871.
16. Martin, R. L., J.-H. Lee, L. L. Cribbs, E. Perez-Reyes, and D. A. Hanck. 2000. Mibefradil block of cloned T-type calcium channels. *J. Pharmacol. Exp. Ther.* **295**: 302–308.
17. Nilius, B., P. Hess, J. B. Lansmann, and R. W. Tsien. 1985. A novel type of cardiac calcium channel in ventricular cells. *Nature* **316**: 440–443.
18. Perez-Reyes, E. 1998. Molecular characterization of a novel family of low voltage-activated, T-type calcium channels. *J. Bioenerg. Biomemb.* **30**: 313–318.
19. Perez-Reyes, E., L. L. Cribbs, A. Daud, A. E. Lacerda, J. Barclay, M. P. Williamson, M. Fox, M. Rees, and J.-H. Lee. 1998. Molecular characterization of a neuronal low voltage-activated T-type calcium channel. *Nature* **391**: 896–900.
20. Randall, A. D. and R. W. Tsien. 1997. Contrasting biophysical and pharmacological properties of T-type and R-type calcium channels. *Neuropharmacology* **36**: 879–893.
21. Shin, S. Y., J. H. Lee, S. H. Huh, Y. S. Park, J. M. Kim, and I. S. Kong. 2000. Overexpression and characterization of *Vibrio mimicus* metalloprotease. *J. Microbiol. Biotechnol.* **10**: 612–619.
22. Steriade, M. and R. R. Llinas. 1988. The functional states of the thalamus and the associated neuronal interplay. *Physiol. Rev.* **68**: 649–742.